

# Effect Of Gamma And Electron Irradiation On The Optical Characteristics Of MgF<sub>2</sub> Crystals And Ceramics

**Malika Anvarovna Mussaeva<sup>1</sup>**

<sup>1</sup>Institute of Nuclear Physics, Academy of Sciences of the Republic of Uzbekistan, Tashkent, Ulugbek settlement, 100214; E-mail: [mussaeva@inp.uz](mailto:mussaeva@inp.uz)

**Mubinaxon Burxon kizi Sobirjonova<sup>2</sup>**

<sup>2</sup>National University of Uzbekistan, Mirzo Ulugbeka, Tashkent, Uzbekistan, 100174.

## ABSTRACT

This paper examines the effects of  $\gamma$ -ray and electron irradiation on the optical properties of MgF<sub>2</sub> crystals and ceramics. The samples were irradiated with  $\gamma$ -rays over a wide dose range and with a 4 MeV electron beam in the fluence range of  $10^{14}$ – $10^{15}$  cm<sup>-2</sup>. A combination of methods was used to study the opaque ceramic samples, including optical and infrared transmission and reflectance measurements, elemental and phase composition analysis, determination of the crystal structure of the near-surface layer, and scanning electron microscopy. For the first time, a deviation in the stoichiometric composition of the near-surface layer of fluoride materials after irradiation was detected using two independent methods-local elemental analysis using characteristic X-rays and IR spectroscopy. The appearance of oxygen in the surface layer was established, which may be related to radiation-induced processes leading to fluorine loss and changes in the chemical composition of MgF<sub>2</sub>. The obtained results expand our understanding of the mechanisms of radiation-induced defect formation and modification of the optical properties of MgF<sub>2</sub> crystals and ceramics.

## Keywords:

MgF<sub>2</sub> crystals, MgF<sub>2</sub> ceramics,  $\gamma$ -irradiation, electron irradiation, optical properties, radiation defects.

## Introduction

Magnesium fluoride (MgF<sub>2</sub>) crystals are important solid-state optical materials widely used in the vacuum ultraviolet, visible, and infrared spectral regions due to their high optical transparency, radiation resistance, and chemical stability [1]. These properties determine their use in spectroscopy, laser technology, optical windows, and radiation transmission elements [2–4]. Doped MgF<sub>2</sub> crystals are used as active media in tunable lasers, especially in the infrared region of the

spectrum, due to the peculiarities of their crystalline structure and low level of optical losses [2,5]. In addition, MgF<sub>2</sub> is widely used as substrates for semiconductor and functional optical materials, as well as in the form of protective and antireflective coatings [3,6]. In recent decades, MgF<sub>2</sub> - based transparent optical ceramics have attracted considerable interest. These ceramics, in terms of a number of characteristics-such as transparency, mechanical strength, and radiation resistance-approach those of single crystals, and in some

cases, offer significant technological advantages associated with scalable production and high property homogeneity [2,6,8]. This makes  $\text{MgF}_2$  ceramics a promising material for use in environments exposed to intense radiation. Exposure to ionizing radiation, particularly  $\gamma$ -quanta and fast electrons, results in the formation of radiation defects in the  $\text{MgF}_2$  crystal lattice, including F-centers,  $\text{F}_2$ -centers, and more complex aggregate defects, which significantly affect the optical and spectral characteristics of the material [1,5,7]. Such defects cause changes in the transmittance, the appearance of radiation absorption bands, and modification of the luminescent properties, the parameters of which depend on the type of radiation, the absorbed dose, and the structural state of the material [7,9]. Despite the existence of a number of studies devoted to radiation effects in  $\text{MgF}_2$  single crystals [1,5,7], as well as studies of optical ceramics based on it [2-4,8], comparative studies of the influence of  $\gamma$ - and electron irradiation on the optical properties of both  $\text{MgF}_2$  crystals and ceramics remain limited. In particular, the role of radiation-induced defects in the formation of the spectral characteristics of materials of different morphologies has been insufficiently studied.

In this regard, the aim of this work is a comparative analysis of the influence of  $\gamma$ - and electron irradiation on the optical properties of  $\text{MgF}_2$  crystals and ceramics, as well as determining the role of radiation defects in the formation of their spectral characteristics.

### Research Objects and Methods.

**Objects.** The objects of study were opaque  $\text{MgF}_2$ -based ceramics with a diameter of 15 mm and a thickness of 2.8 mm,  $\text{MgF}_2$  crystals with dimensions of  $8 \times 8 \times 5$  mm, and pure and nickel-doped  $\text{MgF}_2$  ceramics with dimensions of  $10 \times 10 \times 3$  mm.  $\text{MgF}_2$  crystals and ceramics are classified as wide-bandgap scintillator matrices. Because these microceramics are translucent, the same spectral and structural methods used for microcorundum ceramics were applied to their studies. The samples were obtained by hot pressing magnesium fluoride ( $\text{MgF}_2$ ). Before measurements, the samples were annealed to burn off residual plasticizer added during

sample preparation. Heating to a temperature of  $600^\circ\text{C}$  lasted 50 minutes. The samples were maintained at the maximum temperature for an hour. Cooling of the crystals to room temperature took 1 hour 50 minutes. The samples under study became somewhat discolored as a result of annealing.

**Gamma irradiation.** Samples were irradiated with  $\gamma$ -quanta (1.17 and 1.33 MeV) of the  $^{60}\text{Co}$  isotope using a setup at a rate of 130 R/s in a dose range of  $10^6$ – $10^9$  R at a temperature of 300 K.

**Electron irradiation.** Samples were irradiated at room temperature at the Elektronika U-003 electron accelerator with a normal incidence angle of a constant-density electron beam on the target at fluences ranging from  $10^{14}$  to  $10^{15}$  el/cm<sup>2</sup>.

**Research methods.** The spectral characteristics of the samples were studied using optical and infrared spectroscopy. UV-visible absorption spectra were recorded using a Shimadzu UV-3600 dual-beam spectrophotometer (Japan) in the wavelength range of 190–3300 nm at room temperature. Infrared spectra were obtained on a Nicolet iS50 Fourier transform IR spectrometer (Thermo Scientific, USA) in the mid-infrared range of  $4000$ – $400$  cm<sup>-1</sup>. The surface morphology and elemental composition of the samples were studied by scanning electron microscopy using an EVO MA10 microscope (Carl Zeiss, Germany) equipped with an energy-dispersive X-ray microanalysis (EDX) system. Electron microscopic images were recorded at various magnifications, which made it possible to analyze the surface microstructure. The surface topography and nanoscale characteristics of the samples were investigated by atomic force microscopy using an SPM-9700HT atomic force microscope.

### Results and Discussion.

Figures 1 a) and 1 b) show a surface micrograph and a local characteristic X-ray emission spectrum of an  $\text{MgF}_2$  sample after annealing at  $600^\circ\text{C}$ . As can be seen from the micrograph (Fig. 1a), the surface of the sample after heat treatment is characterized by a

relatively uniform morphology without pronounced macrodefects, indicating the stability of the  $\text{MgF}_2$  structure at this annealing temperature. The table presents the results of a local elemental analysis of the  $\text{MgF}_2$  sample. In the spectrum (Fig. 1 b), magnesium is

represented by two characteristic lines,  $K_{\alpha}$  (1.253 keV) and  $K_{\beta}$  (1.302 keV), while fluorine has one main characteristic line located near the K - line of oxygen. This complicates the correct separation of the contributions of these elements in energy-dispersive analysis.

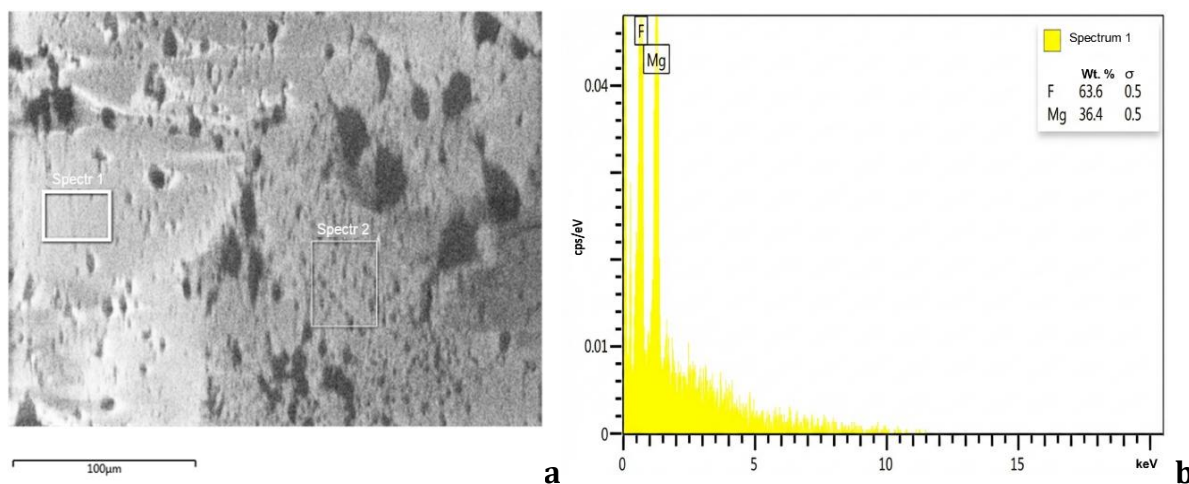


**Fig. 1.** Microphotograph of the surface (a) and local spectrum of characteristic radiation (b) of  $\text{MgF}_2$  after annealing at 600 °C

Table Local elemental composition of  $\text{MgF}_2$

Element	Line type	Stoichiometry composition	Spectrum 1 Wt.%	Error Weight %	Spectrum 2 Wt.%	Error Weight %	Name of the standard
F	K series	61	63.64	0.53	63.43	0.35	$\text{CaF}_2$
Mg	K series	39	36.36	0.53	36.57	0.35	$\text{MgO}$

The stoichiometric composition of  $\text{MgF}_2$ , calculated based on atomic masses ( $M = 24.3 + 2 \times 19 = 62.3$ ), corresponds to a content of approximately 39% Mg and 61% F (by mass). However, local analysis results show an excess of fluorine compared to the calculated stoichiometry.

The likely cause of this discrepancy is the presence of oxygen in the surface layer of the sample, which is associated with annealing at 600 °C in air and possible surface oxidation. This is further confirmed by the spectrum shown in Figure 1b, which shows a contribution from

weak scattering intensity, as well as more intense narrow peaks of boron (0.183 keV) and carbon (0.277 keV), which are poorly resolved. Additionally, a peak of possible oxygen impurity with an energy of approximately 0.525 keV is detected, located near the fluorine peak (0.677 keV). It should be noted that the INCA software interpreted the recorded signals as belonging to elements with the formula  $\text{MgF}_2$ , which may lead to an overestimation of the fluorine content in the presence of overlapping oxygen lines. Thus, the obtained results indicate that annealing of  $\text{MgF}_2$  at a temperature of 600 °C in

an air atmosphere can lead to the formation of an oxygen-containing surface layer, which must be taken into account when interpreting energy

dispersive analysis data and assessing the stoichiometric composition of the samples. Scanning electron microscopy of the  $\text{MgF}_2$  surface is shown in Fig. 2. a, b, c, d.

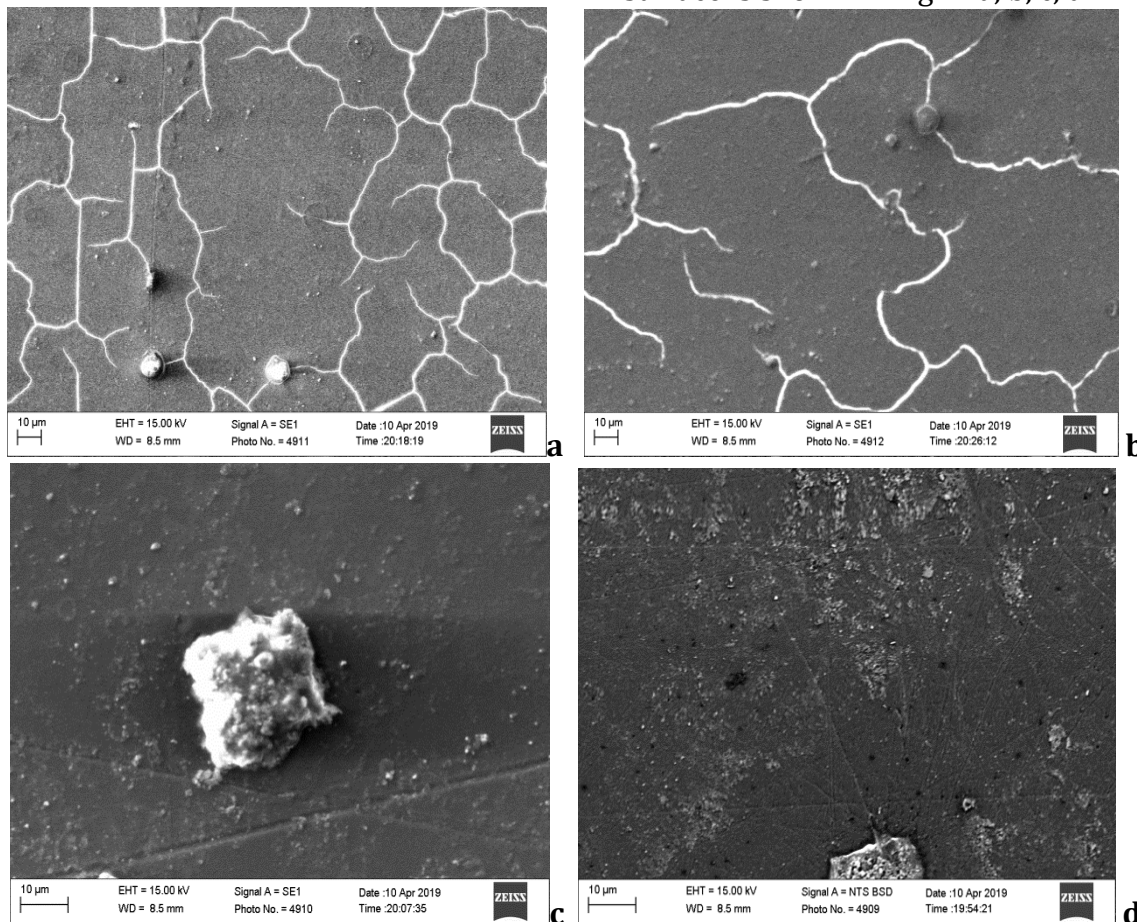


**Fig. 2.** Scanning electron microscopy of the surface of  $\text{MgF}_2$

The micrograph clearly shows bright lines corresponding to the interfaces between the crystalline blocks of irradiated  $\text{MgF}_2$ . Fluorine likely migrated and escaped along these interfaces under the influence of irradiation, leading to local enrichment of the surface with metallic magnesium. Large and small protrusions ("hillocks") are also observed on the surface, which can be attributed to

radiation-induced crystallites formed as a result of defect redistribution and stress relaxation in the surface layer of the material. The large growth is  $\text{CaCO}_3$ , a crystallite from coated paper.

Figure 3 shows the reflection spectra of  $\text{MgF}_2$  crystals gamma-irradiated with different doses from  $10^6$  to  $10^9$  R.

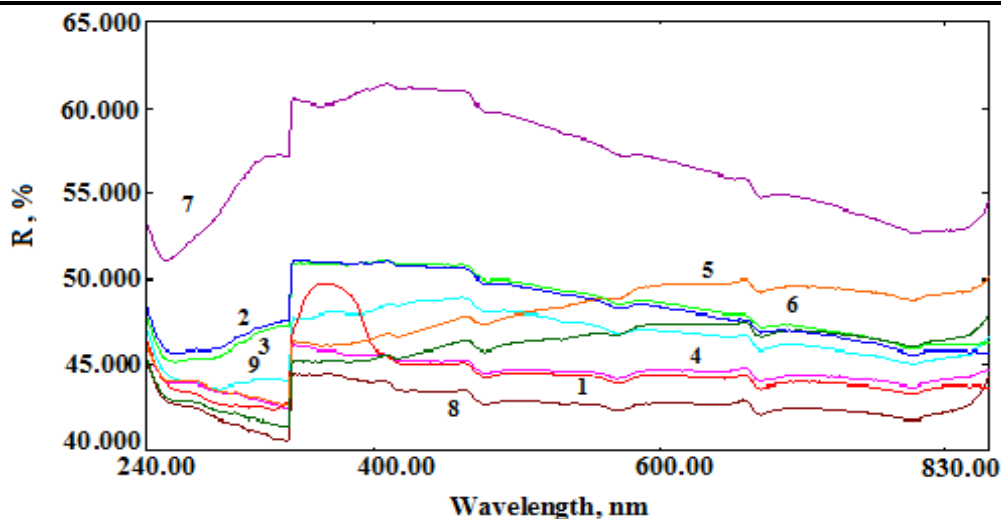
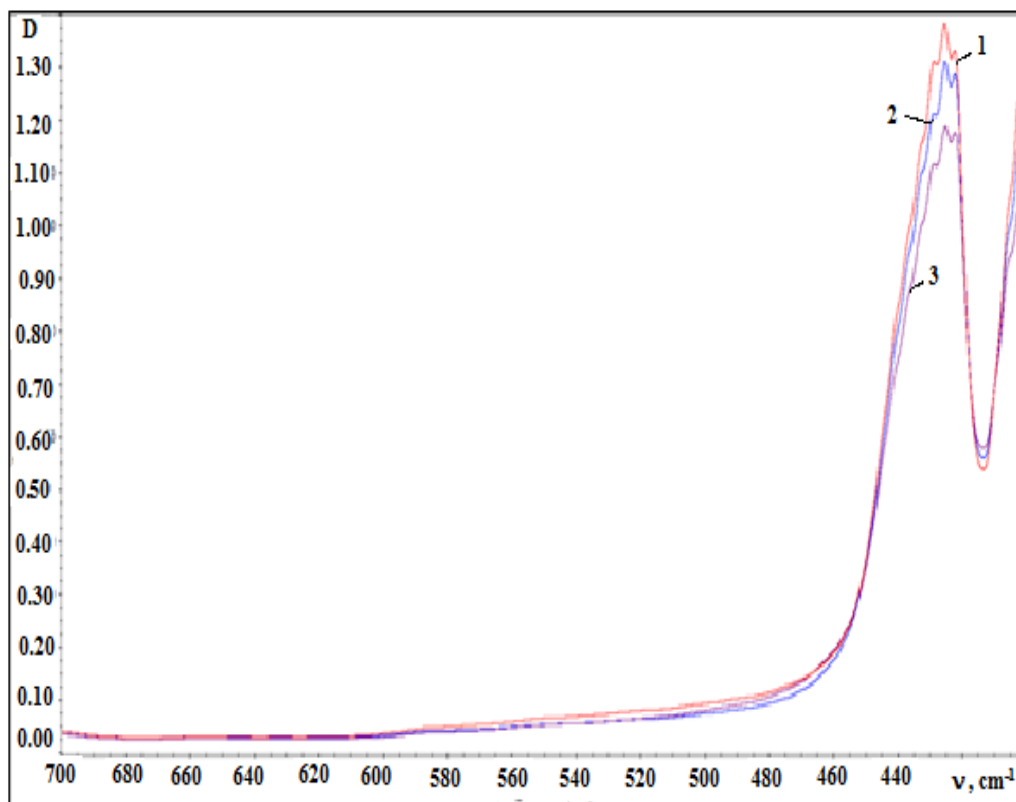


**Fig. 3.** Reflectance spectra of a 5 mm thick  $\text{MgF}_2$  crystal (1 – red) and 1-3 mm thick ceramics, gamma-irradiated with different doses:  $10^6$  R (2 – blue);  $10^7$  R (3 – light green);  $2 \times 10^8$  R (4 – pink);  $2 \times 10^8$  R (5 – orange); 1 mm  $2 \times 10^9$  R (6 – green); 3 mm  $2 \times 10^9$  R (7 – violet); 3 mm  $10^7$  R (8 – brown); 3 mm  $10^7$  R (9 – light blue)

Only in unirradiated  $\text{MgF}_2$  crystals is a selective reflectance band at 370 nm clearly visible. After gamma irradiation over the aforementioned wide (three orders of magnitude) dose range, this band initially disappears.

Then, the UV bands (240–300 nm) and the red band (700 nm) begin to increase. At  $10^8$ – $10^9$  R, the reflectance becomes large and broadband, similar to that of metallic

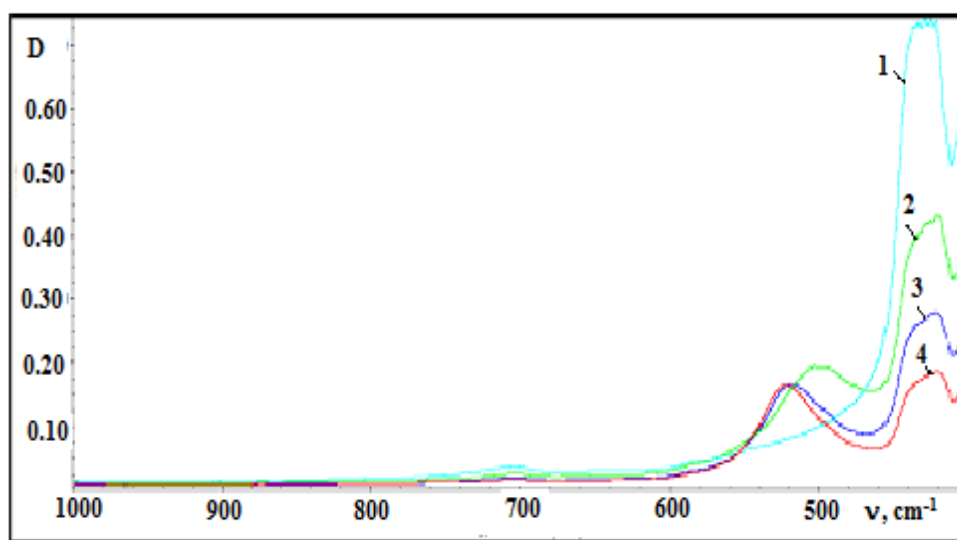
magnesium. This suggests that the Mg-F chemical bond is broken, as is commonly believed, by the loss of fluorine during radiolysis, and the remaining magnesium, in non-stoichiometric excess, forms metallic clusters and even a metallic film. A direct method for studying chemical bonds is infrared absorption. To isolate the surface contribution, a special mode-attenuated total internal reflection-is used, as shown in Figs. 4–6.



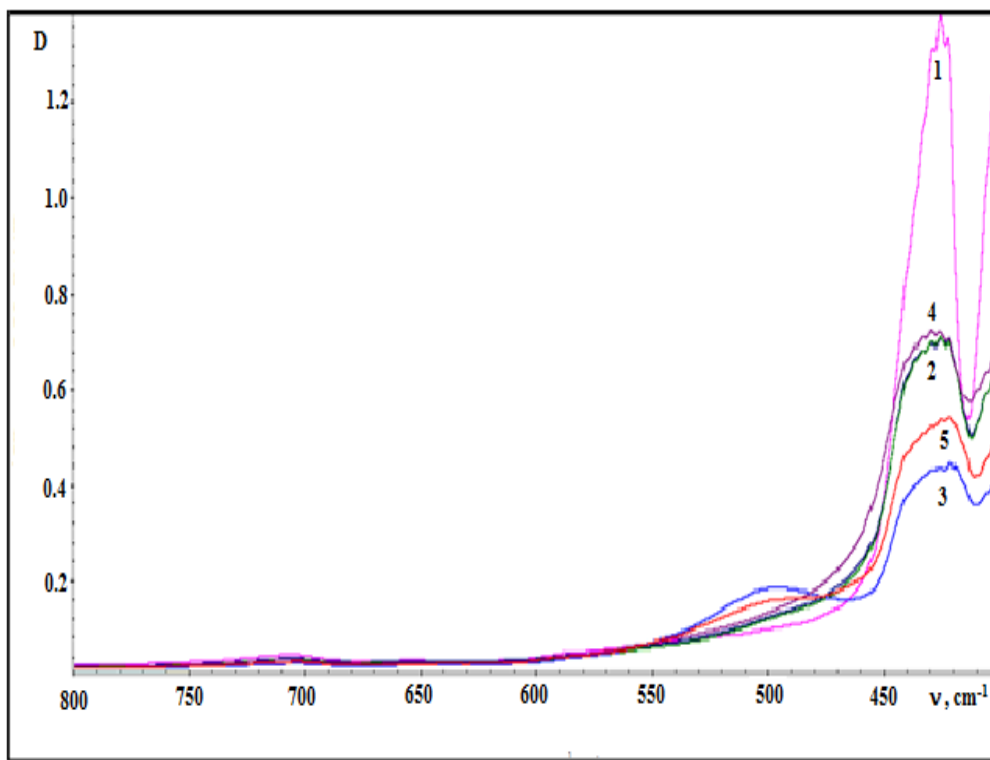
**Fig. 4.** IR absorption of  $\text{MgF}_2$  crystal: 1 – unirradiated; 2 – annealing for 1 hour at  $600\text{ }^\circ\text{C}$  in air; 3 – irradiation in air with 4 MeV electrons, dose  $10^{15}\text{ cm}^{-2}$

The figure shows that after annealing and irradiation, the basic symmetric and asymmetric stretching modes in the  $440\text{--}430\text{ cm}^{-1}$  bands and the bending modes in the  $400\text{--}410\text{ cm}^{-1}$  bands of the Mg-F bond are noticeably

weakened while maintaining the mode frequencies, while the defect peaks ( $415\text{ cm}^{-1}$ , the others in the  $100\text{--}300\text{ cm}^{-1}$  region are not visible) are still very weak. This indicates damage to the lattice in the near-surface layer.



**Fig. 5.** IR absorption of MgF<sub>2</sub> ceramics: 1 – after annealing at 600 °C, 2 – electron irradiation 10<sup>14</sup> cm<sup>-2</sup> 1 MR, 3 – gamma irradiation 10 MR, 4 – gamma irradiation 200 MR



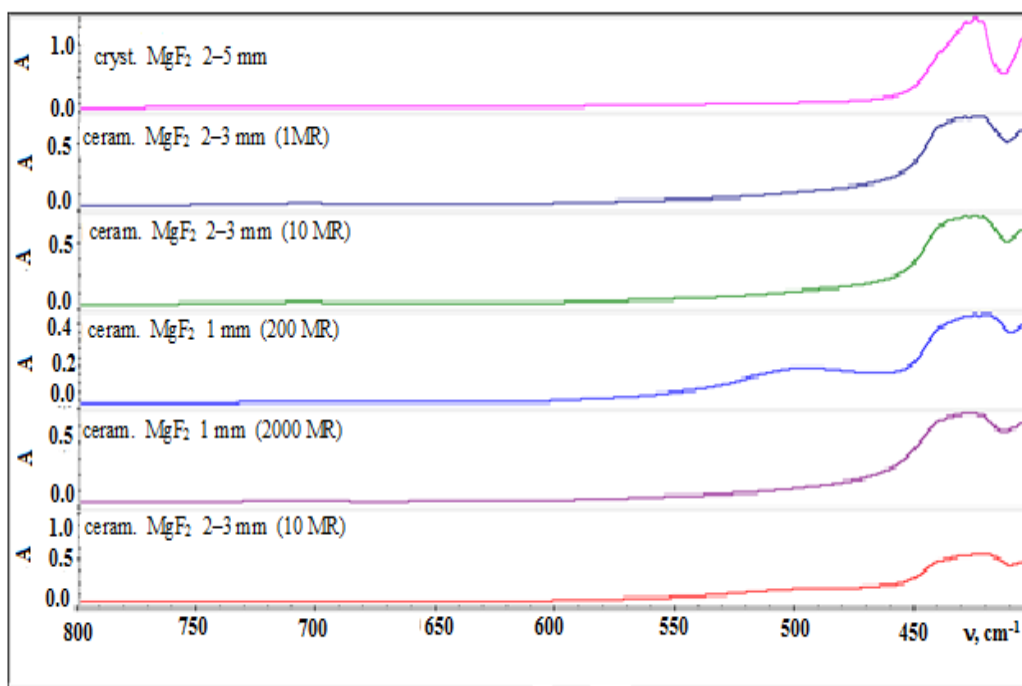


**Fig. 6.** IR absorption of MgF<sub>2</sub> crystal 5 mm thick and ceramics 1–3 mm thick after gamma irradiation with doses from 10<sup>6</sup> to 2×10<sup>9</sup> R in air at 320–350 K

In ceramics, unlike crystals, after irradiation, a significant weakening and broadening of the basic IR vibrations is observed, as well as the appearance of an additional band around 500 cm<sup>-1</sup>, which slowly increases with increasing dose by several orders of magnitude.

### Conclusion

MgF<sub>2</sub> crystals and ceramics were irradiated with gamma rays at various doses and by a 4 MeV electron beam with fluences in the range of 10<sup>14</sup>–10<sup>15</sup> cm<sup>-2</sup>. For opaque ceramics, a combination of methods was used: optical and IR transmittance/reflectance measurements, determination of the elemental and phase composition and crystal structure of the near-surface layer, and scanning electron microscopy. It was shown that at high doses, when the UV absorption bands are saturated, optical and IR reflectance spectroscopy are more informative. Weak peaks of single F and dimeric F<sub>2</sub> centers induced by electron or gamma irradiation were identified in the IR spectra. It is assumed that the electron centers accumulate as fluorine molecules (F<sub>2</sub>) in the interstitial sites. Since the fluorine molecules are small and the rutile

lattice is loose, lattice deformation is minimal, as is the cross section for interactions with other centers.

### Acknowledgement

The authors express their gratitude to the chief researcher of the Institute of Nuclear Physics of the Academy of Sciences of the Republic of Uzbekistan, Doctor of Physical and Mathematical Sciences, Professor E.M. Ibragimova for providing the IR and EDS spectra.

The researches are supported by basic funding allocated to the Institute of Nuclear Physics of the Academy of Sciences of the Republic of Uzbekistan by the decree PP-4526.

### References

1. Facey O.E., Lewis D.L., Sibley W.A. Electron and neutron damage in MgF<sub>2</sub> crystals: Optical absorption and defect formation. *Phys. Status Solidi B* **32** (1969), pp.831–837. <https://doi.org/10.1002/pssb.19690320237>

2. Nakamura F., Kato T., Okada G., Yanagida T. Scintillation, thermally stimulated luminescence and radiophotoluminescence properties of MgF<sub>2</sub> transparent ceramic and single crystal. *Ceram. Int.* **43** (2017), pp.7211–7215.  
<https://doi.org/10.1016/j.ceramint.2017.03.009>
3. Nakamura F., Kato T., Okada G., et al. Scintillation, dosimeter and optical properties of MgF<sub>2</sub> transparent ceramics doped with Gd<sup>3+</sup>. *Mater. Res. Bull.* **98** (2018), pp.83–88.  
<https://doi.org/10.1016/j.materresbull.2017.09.058>
4. Nakamura F., Kato T., Okada G., Kawaguchi N., Fukuda K., Yanagida T. Scintillation and thermally stimulated luminescence properties of MgF<sub>2</sub> transparent ceramics doped with Eu<sup>2+</sup> synthesized by spark plasma sintering. *J. Alloys Compd.* **726** (2017), pp.67–73.  
<https://doi.org/10.1016/j.jallcom.2017.07.320>
5. Sergeev A.P., Sergeev P.B. Individual induced absorption bands in MgF<sub>2</sub>: Correlation with radiation-induced defects. *Quantum Electron.* **38** (2008), pp.251–257.  
<https://doi.org/10.1070/QE2008v038n03ABEH013555>
6. Quesnel E., Dumas L. Optical and microstructural properties of MgF<sub>2</sub> UV coatings grown by ion beam sputtering. *J. Vac. Sci. Technol. A* **18** (2000), pp.2869–2876.  
<https://doi.org/10.1116/1.1318073>
7. Williams G.P., Marquardt C.L., Williams J.W., Kabler M.N. Transient absorption and luminescence in MgF<sub>2</sub> following electron pulse excitation. *Phys. Rev. B* **15** (1977), pp.5003–5011.  
<https://doi.org/10.1103/PhysRevB.15.5003>
8. Li X., Hu C., Liu Q., Hreniak D., Li J. Fluoride transparent ceramics for solid-state lasers: A review. *J. Adv. Ceram.* **13** (2024), pp. 1891–1918.  
<https://doi.org/10.26599/jac.2024.9220986>
9. Farouka M., Fayek S.A., Ibrahim M., Okr M.E. Effect of  $\gamma$ -irradiation on optical absorption of Al<sub>2</sub>O<sub>3</sub>-TeO<sub>2</sub>-Li<sub>2</sub>B<sub>4</sub>O<sub>7</sub> glasses doped with MgF<sub>2</sub>. *Ann. Nucl. Energy* **56** (2013), pp.39–43.  
<https://doi.org/10.1016/j.anucene.2013.01.019>